Downloaded from genome.cshlp.org on July 16, 2026 . Published by Cold Spring Harbor Laboratory Press

Estimating absolute methylation levels at single CpG resolution from methylation enrichment and restriction enzyme sequencing methods

Michael Stevens, Jeffrey B Cheng, Daofeng Li, et al.

Genome Res. published online June 26, 2013
Access the most recent version at doi:10.1101/gr.152231.112

P<P Published online June 26, 2013 in advance of the print journal.

Accepted Manuscript Peer-reviewed and accepted for publication but not copyedited or typeset; accepted manuscript is likely to differ from the final, published version.

Creative Commons License This article is distributed exclusively by Cold Spring Harbor Laboratory Press for the first six months after the full-issue publication date (see http://genome.cshlp.org/site/misc/terms.xhtml). After six months, it is available under a Creative Commons License (Attribution-NonCommercial 3.0 Unported), as described at http://creativecommons.org/licenses/by-nc/3.0/.

Email Alerting Service Receive free email alerts when new articles cite this article - sign up in the box at the top right corner of the article or **click here.**

To subscribe to *Genome Research* go to:
https://genome.cshlp.org/subscriptions

© 2013, Published by Cold Spring Harbor Laboratory Press

Downloaded from genome.cshlp.org on July 16, 2026 . Published by Cold Spring Harbor Laboratory Press

Submission to Genome Research as Methods

Title: Estimating Absolute Methylation Levels at Single CpG Resolution from Methylation Enrichment and Restriction Enzyme Sequencing Methods

Running title: methylCRF predicts single CpG resolution methylome

Michael Stevens[1,2], Jeffrey B. Cheng[3], Daofeng Li[1], Mingchao Xie[1], Chibo Hong[4], Cécile L. Maire[5], Keith L. Ligon[5,6], Martin Hirst[7,8], Marco A. Marra[7], Joseph F. Costello[4], Ting Wang[1,2]

[1] Department of Genetics, Center for Genome Sciences and Systems Biology, Washington University School of Medicine, St. Louis, MO 63108

[2] Department of Computer Science and Engineering, Washington University in St. Louis, St. Louis, MO 63130

[3] Department of Dermatology, University of California San Francisco, CA 94143

[4] Brain Tumor Research Center, Department of Neurosurgery, Helen Diller Family Comprehensive Cancer Center, University of California San Francisco, CA 94143

[5] Department of Medical Oncology, Center for Molecular Oncologic Pathology, Dana-Farber Cancer Institute, Boston, MA 02215

[6] Departments of Pathology, Brigham and Women's Hospital, Boston Children's Hospital, and Harvard Medical School, Boston, MA 02115

[7] BC Cancer Agency, Canada's Michael Smith Genome Sciences Centre Vancouver, British Columbia, Canada.

[8] Department of Microbiology and Immunology, University of British Columbia, Vancouver, British Columbia, Canada

Correspondence should be addressed to J.F.C (jcostello@cc.ucsf.edu) or T.W. (twang@genetics.wustl.edu).

Keywords: DNA methylation, Conditional Random Fields, Epigenomics

Downloaded from genome.cshlp.org on July 16, 2026 . Published by Cold Spring Harbor Laboratory Press

ABSTRACT

Recent advancements in sequencing-based DNA methylation profiling methods provide an unprecedented opportunity to map complete DNA methylomes. These include whole genome bisulfite sequencing (WGBS, MethylC-seq, or BS-seq), Reduced-Representation Bisulfite-Sequencing (RRBS), and enrichment-based methods such as MeDIP-seq, MBD-seq, and MRE-seq. These methods yield largely comparable results, but differ significantly in extent of genomic CpG coverage, resolution, quantitative accuracy, and cost, at least while using current algorithms to interrogate the data. None of these existing methods provides single-CpG resolution, comprehensive genome-wide coverage, and cost feasibility for a typical laboratory. We introduce methylCRF, a novel Conditional Random Fields-based algorithm that integrates methylated DNA immunoprecipitation (MeDIP-seq) and methylation-sensitive restriction enzyme (MRE-seq) sequencing data to predict DNA methylation levels at single CpG resolution. Our method is a combined computational and experimental strategy to produce DNA methylomes of all 28 million CpGs in the human genome for a fraction (<10%) of the cost of whole genome bisulfite sequencing methods. methylCRF was benchmarked for accuracy against Infinium arrays, RRBS, WGBS sequencing, and locus specific-bisulfite sequencing performed on the same human embryonic stem cell line. methylCRF transformation of MeDIP-seq/MRE-seq was equivalent to a biological replicate of WGBS in quantification, coverage and resolution. We used conventional bisulfite conversion, PCR, cloning and sequencing to validate loci where our predictions do not agree with whole genome bisulfite data, and in 11 out of 12 cases methylCRF predictions of methylation level agree better with validated results than does whole genome bisulfite sequencing. Therefore, methylCRF transformation of MeDIP-seq/MRE-seq data provides an accurate, inexpensive and widely accessible strategy to create full DNA methylomes.

Downloaded from genome.cshlp.org on July 16, 2026 . Published by Cold Spring Harbor Laboratory Press

INTRODUCTION

The haploid human genome contains approximately 28 million CpGs that exist in methylated, hydroxymethylated, or unmethylated states. The methylation status of cytosines in CpGs influences protein-DNA interactions, gene expression, and chromatin structure and stability, and plays a vital role in the regulation of cellular processes including host defense against endogenous parasitic sequences, embryonic development, transcription, X chromosome inactivation, and genomic imprinting, as well as possibly playing a role in learning and memory (Robertson 2005; Suzuki and Bird 2008; Laird 2010; Jones 2012). Understanding the role of DNA methylation in development and disease requires accurate assessment of the genomic distribution of these modifications (Laird 2010). Recent advancements in sequencing-based DNA methylation profiling methods provide an unprecedented opportunity to map complete DNA methylomes. Techniques for high throughput detection of cytosine methylation include bisulfite conversion of unmethylated cytosines to uracil, immunoprecipitation with antibodies specific for methylated DNA, and cleavage of CpG containing restriction sites by methylation sensitive or methylation-dependent restriction endonucleases followed by sequencing or microarray hybridization (Bock 2012).

The most comprehensive method, bisulfite treatment followed by sequencing, (whole genome bisulfite sequencing, or WGBS, including MethylC-seq (Lister et al. 2009) and BS-seq (Cokus et al. 2008; Laurent et al. 2010)), measures single cytosine methylation levels genome-wide and directly estimates the ratio of molecules methylated rather than enrichment levels. However this method requires essentially re-sequencing the entire genome multiple times for every experiment (with up to half the reads not even covering CpG sites). To obtain a complete DNA methylome, the total sequencing depth required for adequate coverage of each strand is equivalent to 30X of the human genome (90Gb) which remains an expensive experiment. In addition to its high cost, bisulfite converted genomes have lower sequence complexity and reduced GC content. Therefore, performance of WGBS based methods is also influenced by potential differences in the efficiency of amplification of methylated and unmethylated DNA copies of the same locus, and the ability to accurately align bisulfite converted sequencing reads to the genome, which is more challenging than alignment of conventional reads (Krueger et al. 2012). As noted, 10% of CpGs in the mammalian genome remain refractory to alignment of bisulfite-converted reads (Laird 2010).

Reduced Representation Bisulfite-Sequencing (RRBS) (Meissner et al. 2008) addresses the cost issue by measuring single CpG methylation only in CpG dense regions. For the human

Downloaded from genome.cshlp.org on July 16, 2026 . Published by Cold Spring Harbor Laboratory Press

genome, it requires only around 3Gb of sequencing to achieve the same degree of sequencing depth for most regions of interest. However, RRBS's ability to interrogate a locus is dependent on its MspI cut-site (CCGG) density and consequently measures 10-15% of the CpGs in the human genome (Bock et al. 2010; Harris et al. 2010).

Restriction enzyme methods (e.g. MRE-seq (Maunakea et al. 2010)), on the other hand, typically incorporate parallel digestions with 3-5 restriction endonucleases. Utilizing multiple cut-sites, MRE-seq can cover close to 30% of the genome and saturates at ~3 Gb of sequencing (Nair et al. 2011). These methylation-sensitive enzymes cut only restriction sites with unmethylated CpGs and each read indicates the status of a single CpG. While methylated CpG's could be inferred by the absence of reads at cutting sites, this would require assuming perfect digestion that is not typically done in practice.

In contrast to MRE-seq, methods utilizing monoclonal antibodies against 5-methylcytosine (MeDIP-seq) (Weber et al. 2005; Maunakea et al. 2010) or methylated DNA-binding proteins (MBD-seq, domains of MBD2 alone, or in combination with MBD3L) (Serre et al. 2009), to enrich for methylated DNA independent of DNA sequence have been estimated to saturate at 5 Gb of sequencing (Nair et al. 2011). An important advantage of MeDIP over restriction enzyme methods is a lack of bias for a specific nucleotide sequence, other than CpGs. However, the relationship of enrichment to absolute methylation levels is confounded by variables such as CpG density (Pelizzola et al. 2008). Another inherent limitation of MeDIP-seq in its current form is its lower resolution (~150bp) compared to MRE-seq or bisulfite-based methods in that one or more of the CpGs in the immunoprecipitated DNA fragment could be responsible for the antibody binding.

Finally, array-based platforms are widely utilized. Approaches which couple bisulfite conversions with hybridization-based arrays (e.g. Illumina's HumanMethylation450 BeadChip arrays), while having single base pair resolution, are limited to *a priori* targeted regions. For example, the Illumina BeadChip array assesses methylation at ~485K targeted CpGs, averaging 17 CpGs per gene spread across CpG islands and gene loci. (For this analysis we also utilized the previous BeadChip version which contains 27K CpGs.)

As sequencing costs drop, the number of complete single nucleotide DNA methylome maps is increasing, however, still only a few are publicly available for human. Barring a disruptive technological advance, the need for DNA methylome maps to address fundamental biological questions will likely continue to far outpace the production of new maps for years. In contrast, many more lower-cost DNA methylomes of either lower resolution or lower coverage have been generated across diverse biological and disease states. For example, the NIH Roadmap

Downloaded from genome.cshlp.org on July 16, 2026 . Published by Cold Spring Harbor Laboratory Press

Epigenomics Project's current release of the Human Epigenome Atlas (Bernstein et al. 2010) contains 8 WGBS datasets, 119 RRBS datasets, 49 MeDIP-seq and 45 MRE-seq datasets. These methods yield largely comparable results, but differ significantly in extent of genomic CpG coverage, resolution, quantitative accuracy, and cost, at least using current algorithms to interrogate the data (Bock et al. 2010; Harris et al. 2010). None of these existing methods provides single-CpG resolution, comprehensive genome-wide coverage, and a cost that is affordable for a typical laboratory, particularly when many samples are assayed. To address these needs we describe here methylCRF, a novel Conditional Random Fields-based algorithm that integrates methylated DNA immunoprecipitation (MeDIP-seq) and methylation-sensitive restriction enzyme (MRE-seq) sequencing data to predict DNA methylation levels at single CpG resolution.

RESULTS

Motivation for integrating MeDIP-seq and MRE-seq data

MeDIP-seq and MRE-seq provide complementary readouts of DNA methylation (Maunakea et al. 2010). Their protocols are simple and differ in important ways from bisulfite treatment methods (Harris et al. 2010; Maunakea et al. 2010). By using simple heuristics, the combination of these two methods gave promising results in identifying differentially methylated regions (DMRs) and intermediate or mono-allelic methylation (Harris et al. 2010). Here we further explore the complementary nature of MeDIP-seq and MRE-seq. All genome-wide DNA methylation profiling methods have their own unique biases which can lead to errors in assessing methylation states. Observed genome-wide measurements (MeDIP-seq, MRE-seq, WGBS, etc) are derived from the actual methylation states of the sample, which is unknown or "hidden" from the investigators. These hidden methylation states are often inferred from the observed data, which are usually sequencing reads aligned to the reference genome. Because MeDIP-seq and MRE-seq are independent, complementary measurements of the same methylation state, our confidence in inferring the methylation state can be significantly increased when results from these two methods are integrated. For example, a decrease in MeDIP-seq signal could reflect a biological event (we infer that this region is unmethylated) or could be a methodological artifact; but if the inferred unmethylated state is corroborated by an increase of MRE-seq signal, then the inference of unmethylation is stronger. Thus, integrating MeDIP-seq and MRE-seq is expected to significantly improve our ability to predict methylation levels accurately.

Downloaded from genome.cshlp.org on July 16, 2026 . Published by Cold Spring Harbor Laboratory Press

While MeDIP-seq and MRE-seq data correlate to a certain degree with WGBS measurements (**Fig. 1A**, **B**), their relationship is not well represented by a simple linear translation. It has also remained technically challenging to infer absolute methylation levels from enrichment measurements alone (Down et al. 2008; Pelizzola et al. 2008; Chavez et al. 2010; Harris et al. 2010). Importantly, existing high-resolution methylomes and prior regional analyses reveal that CpG methylation levels are highly non-random throughout the genome (Lister et al. 2009). The levels vary strongly with local CpG density, display distinct genomic feature-specific characteristics, and show strong correlation between neighboring CpG sites (**Fig. 2A**, **B**, **C**). These properties motivated us to use a formal statistical model to explore these complex relationships with the goal of making an accurate, comprehensive, high-resolution prediction of DNA methylation levels from MeDIP-seq and MRE-seq data.

Summary of the methylCRF algorithm

We chose a Conditional Random Field (CRF) model to integrate MeDIP-seq and MRE-seq data to predict genome-wide single CpG methylation levels. Like the Hidden Markov Model (HMM), which has been extensively adopted by the computational biology field (R. Durbin 1998), CRFs were initially developed for natural language processing (Lafferty et al. 2001) but their application in biological research has been limited (Wallach 2004). However, CRFs have several distinct advantages when modeling data with complex inter-dependencies which is a common feature of biological data.

The primary advantage is due to that CRFs model the conditional probability of the variable of interest (CpG methylation states) given observed variables (e.g. MRE scores and MeDIP scores), whereas HMMs model the joint probability of all model variables (**Fig. 3A**). By conditioning on the observed variables, CRFs are not confounded by correlation between them. This then allows CRFs to efficiently model more complex relationships between CpG methylation levels and larger numbers of potentially correlated and distant observations. In contrast, modeling the full joint probability either requires modeling the inter-dependencies between the observations (for example, between MeDIP-seq read count and CpG density) or making the assumption that they are conditionally independent (**Fig. 3B**) – which in this case, they are not (Pelizzola et al. 2008). Since very little is actually known about possible additional confounding factors in these assays, this construction gives us significant freedom in choosing what data to use in predicting methylation levels. Considering the number of features that may influence CpG methylation, we believe this is a critical benefit. This also allows the dependency of the methylation ratio of a CpG on any single observation or groups of observations anywhere

Downloaded from genome.cshlp.org on July 16, 2026 . Published by Cold Spring Harbor Laboratory Press

in the genome to be accounted for with the model complexity growing only by feature number and not by distance of the dependency as would happen in a HMM. Long range-interactions are a common problem (DeCaprio et al. 2007; Yin and Li 2010). Of note, a CpG's methylation ratio can depend on observations in both directions which would introduce loops in a HMM. Additionally, by not having to consider dependencies between observations, the addition of agglomerative and derivative features is trivial. In our case, this was extremely useful as we could define features incorporating large windows of MeDIP-seq and MRE-seq scores at each CpG without increasing the complexity of the inference and without considering their complicated dependence on individual MeDIP-seq and MRE-seq scores.

An additional, practical benefit of using CRFs is that the specification of the model is created by defining functions in a way that offers great flexibility. In a typical implementation, these functions are then instantiated with every combination of assignments of values for its parameter variables. However, one could instantiate with only one or a subset of the values a variable can take without requiring the addition of a full probability distribution over all of the values. In a large model, this can provide a significant reduction in model complexity. Feature functions can also overlap or use subset of variables of another. While subsetting does not add any expressiveness to the model, it provides an elegant and automated way to handle missing observations as well as to take advantage of a more detailed feature for some configurations of the variables while having a simpler representation for other configurations.

Lastly, since we are only interested in predicting correct methylation levels given our experimental data and the experimental data is fixed at test time, we do not believe there is any sacrifice in power by not modeling the full joint probability distribution. Also note that methylation ratios can be interpreted as a maximum likelihood estimate of the probability of a particular CpG being methylated and as our results indicate this probabilistic interpretation appears effective.

Our complete CRF model, methylCRF, is described in detail in the **Methods** section. Features include MeDIP-seq and MRE-seq measurements covering individual CpGs, distance between neighboring CpGs, distribution of MRE sites, and genomic annotations including CpG islands, genes, repeats, and evolutionary conservation of DNA sequences. We also generated a variety of derived scores representing averaged experimental measurements in genomic windows of different sizes. We trained a separate CRF for each genomic feature, and for the final methylation estimates, we averaged the predictions for any CRF whose predictions overlapped. Training was performed using MethylC-seq (Lister et al. 2009) measured methylation levels in randomly chosen regions representing 20% of the genome (**Supplementary Table 1**). Methylation levels were predicted genome-wide, and performance

Downloaded from genome.cshlp.org on July 16, 2026 . Published by Cold Spring Harbor Laboratory Press

was evaluated using CpGs that were not used for training.

High concordance between methylCRF and WGBS predictions

Using methylCRF, we predicted individual methylation levels of 28 million CpGs for Human H1 Embryonic Stem Cells (ESC) with combined MeDIP-seq and MRE-seq data. Our predictions are in high concordance with MethylC-seq predictions on the same H1 cells, with a genome-wide correlation of 0.77 (**Fig. 4A**). methylCRF recapitulates the bimodal distribution of methylation levels identified by MethylC-seq (**Fig. 4A**). Using a previously developed concordance measurement (defined as the percent of CpGs with a methylation proportion difference less than 0.1 or 0.25)(Harris et al. 2010), methylCRF and MethylC-seq are 91% concordant within a 0.25 difference (**Fig. 4B**). This high concordance is illustrated by a genome-browser comparison between methylCRF and MethylC-seq of a representative genomic locus (**Fig. 4C**).

We next compared methylCRF and MethylC-seq on various genomic features (**Fig. 5A**). methylCRF and MethylC-seq agreed at an exceptionally high level for CpGs within CpG islands, promoters, 5' UTRs, and exons with 93%, 93%, 93%, and 96% respective concordances. The concordance decreased in Repeat-Masker annotated regions and regions with no annotation (**Fig. 5A**), possibly reflecting higher mapping errors in these regions, particularly for the reduced complexity reads from bisulfite conversion.

Benchmarking against other experimental methods

Several additional DNA methylation datasets exist for the H1 ESC line, including data obtained with RRBS and Infinium methylation array. In addition, a WGBS dataset was generated for the H9 human embryonic stem cell line (BS-seq) (Laurent et al. 2010). Data from this closely related ESC line provides the closest "biological replicate" of the MethylC-seq ESC H1 WGBS dataset.

When compared to MethylC-seq, methylCRF's performance is almost indistinguishable the comparison between MethylC-seq and BS-seq on these ESC cell lines (**Fig. 4B, 4C, 5A**). Specifically, within a 28% difference window, per-CpG methylation levels between the MethylC-seq (H1) and BS-seq (H9) are 90% concordant while methylCRF (H1) predictions reach the same concordance with a window of 23%. These windows decrease to 26% for H9 and 18% for methylCRF when we limit the comparison to CpGs with high MethylC-seq (H1) read coverage (e.g. >10 reads) and not in repetitive regions.

Downloaded from genome.cshlp.org on July 16, 2026 . Published by Cold Spring Harbor Laboratory Press

RRBS has comparable concordance levels to methylCRF when compared to MethylC-seq. The Infinium array data appears to have slightly higher concordance, which might be a result of having many fewer (~28,000) CpGs for comparison and/or non-random selection of CpGs on the Infinium platform (**Fig. 4C** and **5A**). The high concordance among these popular methods is consistent with previous comparisons (Bock et al. 2010; Harris et al. 2010). However, these methods clearly interrogate very different fractions of the DNA methylomes, as evidenced by the Genome Browser view (**Fig. 4C**) and CpG coverage comparison (**Fig. 5B**).

Robust performance across a variety of measurements

The strength of WGBS predictions is significantly influenced by sequencing coverage. Previous analyses suggest that the methylation level of individual CpGs can only be confidently estimated when sequencing depth is at least 10 (Harris et al. 2010). Therefore, typically the minimum requirement for a WGBS experiment is to sequence the bisulfite converted genome to a depth of 30X (Krueger et al. 2012). However, even at this sequencing depth, a significant number of CpGs still are not covered by enough reads (**Fig. 6A**). Indeed, we observe increased concordance with increasing MethylC-seq coverage. For example, with a minimum 10-read coverage level the concordance within a 0.25 threshold window between methylCRF and MethylC-seq increased to 93% (from 91%, minimum 1-read coverage)(**Fig. 6A**).

CpG density is a major confounding factor in analyzing methyl-cytosine enrichment based methods (Down et al. 2008; Pelizzola et al. 2008). For example, inferring methylation levels in CpG-poor regions is thought to be highly inaccurate or impossible using MeDIP-seq (Pelizzola et al. 2008). Therefore, we examined methylCRF's performance across regions with differing CpG density and found the concordance between methylCRF and MethylC-seq does not vary significantly based on CpG density **(Fig. 6B**).

We also compared methylCRF with BATMAN (Down et al. 2008), a popular method for analyzing MeDIP-seq data. Since BATMAN predicts methylation levels in windows of fixed-size and not of single CpGs, we assigned each CpG the methylation level of its window. methylCRF consistently outperforms BATMAN in all categories (**Fig. 6D**).

Since our model learns separate CRFs for each genomic feature, we asked if it is possible that the high correlations between methylCRF and MethylC-seq could be explained by each CRF capturing the *a priori* methylation distributions of genomic features instead of using the experimental data. To examine this relationship, we applied methylCRF: 1) without MeDIP-seq data, 2) without MRE-seq data, and 3) with neither MeDIP-seq nor MRE-seq data, i.e. with only genomic features (**Fig. 6C**). The experimental data does indeed make a large difference in our

Downloaded from genome.cshlp.org on July 16, 2026 . Published by Cold Spring Harbor Laboratory Press

predictions. Interestingly, MRE-seq alone performs slightly better than MeDIP-seq alone. This may be due to the ability of a CRF to incorporate *a priori* knowledge that most CpGs are methylated, thus making some MeDIP-seq information redundant. However, it is important to note that the combination of MeDIP-seq and MRE-seq improves performance significantly.

To further demonstrate that experimental data, but not the *a priori* methylation status of genomic features drives our prediction, we compared the rates of concordance for methylated and unmethylated CpG islands. Using MethylC-seq scores for H1 ES cells, we defined 17,189 unmethylated and 6,728 methylated CpG islands with an average methylation level of <=0.2 and >= 0.8 respectively. We compared these with the average methylCRF scores for H1 ES cells for each of these CpG islands (**Fig. 6D**). Clearly, methylCRF predicts similar sets of methylated and unmethylated CpG islands as MethylC-seq and it does both equally well. Furthermore, on a per-CpG level, unmethylated CpG islands concordance is 0.98, while methylated CpG islands concordance is 0.96. This analysis strongly suggests that while we take advantage of *a priori* information, like genomic features, the algorithm clearly integrates experimental data, relationships within the data, and between data and genomic features to make accurate predictions. We performed a similar analysis on the subset of CpG islands located in promoters – that is, a partitioning of CpG islands independent of the model of the CpG island-specific CRF – and obtained similar results (**Supplementary Fig. S1**). Similar results were also obtained when we restricted our analysis to intergenic CpG islands (**Supplementary Fig. S2**).

methylCRF accuracy is robust when applied to a second sample

Having demonstrated that methylCRF can accurately predict differential DNA methylation of CpGs independent of the characteristic methylation status of their genomic feature, we tested whether our model, trained on data from H1 embryonic stem cells, would generalize to data of other samples. This includes testing whether methylCRF can predict differential DNA methylation at a genomic locus between different samples. We reason that if methylCRF is completely dependent on genomic features, or is over-trained with ESC data, we would not be able to distinguish between datasets generated from other cell or tissue types.

We generated WGBS, Infinium HumanMethylation450 BeadChip, MeDIP-seq and MRE-seq data profiles of a human fetal neural stem cells (NSCs) culture (Hu-F-NSC-02, neurosphere cultured cells, ganglionic eminence derived, fetal age of 21 weeks) (**Supplementary Table 1**). We generated a single CpG resolution DNA methylome of this sample using methylCRF. We performed similar concordance analysis between predictions of methylCRF and that of WGBS,

Downloaded from genome.cshlp.org on July 16, 2026 . Published by Cold Spring Harbor Laboratory Press

and between methylCRF and Infinium array. The overall concordance is consistently high for comparison of methylCRF against either WGBS or Infinium arrays (**Fig. 7A**). Specifically, methylCRF and WGBS were 88% concordance within a 0.25 difference window, and 65% concordance within a 0.10 difference window. Additionally, we defined differentially methylated CpG islands between the H1 ESC and the fetal NSCs using the WGBS data. Out of 26,845 CpG islands, we identified 233 that have significantly different methylation status between H1 ESC and fetal NSCs, such that their average methylation levels are less than 0.2 in one sample but greater than 0.8 in the other. These WGBS defined, cell type-specific differences in CpG island methylation were mirrored by similar differences between H1 ESC and fetal NSCs estimated by methylCRF (**Fig. 7B**), suggesting methylCRF can faithfully predict differential DNA methylation between two samples.

Finally, we evaluated the ability of methylCRF to predict intermediate methylation levels. We did not include imprinted control regions (ICRs) as a genomic feature in training. However, when we examined methylation status of known ICRs (obtained from https://atlas.genetics.kcl.ac.uk, and summarized in **Supplementary Table 2**), we found that majority of the ICRs exhibited intermediate methylation levels based on methylCRF prediction in both H1 ESC and fetal NSCs (**Fig. 8A, B**), and the levels were consistent with those determined by WGBS based methods (**Fig. 8A, B**). Genome Browser views of the data were provided for two exemplar ICRs (**Fig. 8C, D**).

Experimental validation

For regions where methylCRF and MethylC-seq results were discordant in H1 ESC, we experimentally validated methylation status by performing PCR amplification of bisulfite converted DNA, followed by Sanger sequencing of cloned amplicon DNA. Out of 12 regions that show disagreement, bisulfite validation agreed better with methylCRF in 11 cases, and agreed better with MethylC-seq in only 1 case. Two of the tested loci are shown in **Figure 9**, while the remaining sites are summarized in **Table 1** and **Supplementary Figure S3**.

DISCUSSION

DNA methylation is an epigenetic mark that has important regulatory roles in a broad range of biological processes and diseases (Jones 2012). Understanding the role of DNA methylation in development and disease requires knowledge of the distribution of these modifications in the

Downloaded from genome.cshlp.org on July 16, 2026 . Published by Cold Spring Harbor Laboratory Press

genome. The technology is now available for studying DNA methylation genome-wide, at high resolution and in a large number of samples (Bock 2012). Previous comparisons suggest that many popular methods yield largely comparable results, but they differ significantly in extent of genomic CpG coverage, resolution, quantitative accuracy, and cost (Bock et al. 2010; Harris et al. 2010), at least using current algorithms to interrogate the data.

We introduce a combined computational and experimental strategy to produce single CpG resolution DNA methylomes of all 28 million CpGs in the human genome at a fraction of the cost of whole genome bisulfite sequencing methods. Our computational model, methylCRF, is based on Conditional Random Fields, a model similar to the well-known Hidden Markov Model, initially developed for natural language processing but less applied in biomedicine. Using this model, we integrated data from two complementary DNA methylation assays (MeDIP-seq and MRE-seq) to predict methylation at single CpG resolution that were similar to the results from WGBS on the DNA of the same cell line. However, the cost of our two assays combined is less than 10% of a whole genome bisulfite sequencing methylome. We showed that methylation levels assessed by methylCRF from MeDIP-seq/MRE-seq data are indistinguishable from a biological replicate of whole genome bisulfite sequencing.

A complete genome-wide DNA methylome of a given sample will describe methylation levels of every CpG in the genome, approximately 28 million in humans. WGBS based method is considered the only approach capable of producing such single CpG resolution DNA methylomes. It is perhaps the most celebrated method in DNA methylomics to date and generally considered superior to enrichment-based methods (Krueger et al. 2012). One important reason that WGBS appears conceptually superior to enrichment-based methods is that transformation of sequencing results to direct estimates of methylation levels of individual CpGs is straightforward – once data is aligned to the reference genome, one can simply count converted and unconverted Cs to infer methylation levels. Although WGBS does not directly measure single CpG methylation levels of a sample, investigators can easily infer methylation levels based on experimental data (by sequencing alleles from multiple cells) derived from the true methylation states, i.e., observed counts of converted and unconverted Cs. Such intuitive heuristics makes WGBS seem straightforward.

Similarly, enrichment-based data are also derived from true methylation states. However, current analytical methods for enrichment-based data usually calculate enrichment scores that are indicative of regional DNA methylation levels corrected by local CpG distribution (Down et al. 2008; Chavez et al. 2010), but do not predict single CpG methylation levels. Our novel algorithm closes this gap – we can predict single CpG methylation levels based on MeDIP-seq and MRE-

Downloaded from genome.cshlp.org on July 16, 2026 . Published by Cold Spring Harbor Laboratory Press

seq data, two fundamentally different methods. The algorithm represents a fundamental advancement in statistical modeling over methods currently applied to enrichment-based methods.

There are still significant barriers to individual laboratories adopting WGBS as a routine assay, mainly the high production cost. Our method costs only a fraction of that of WGBS, yet can achieve comparable results. Importantly, the cost saving is scalable; any anticipated reduction in sequencing cost will reduce the cost of WGBS and our method in equal proportions. We performed saturation analysis of MeDIP and MRE and concluded that ~ 30M MRE reads and 50M MeDIP reads are required to reach saturation for measuring a human DNA methylome (**Supplementary Notes, Supplementary Fig. S4**). This translates to 1-1.5X coverage of the human genome. For WGBS, the requirement is at least 20-30X coverage. This striking 20-fold difference in required coverage will remain unchanged across different next-generation sequencing platforms. To generate 30X coverage for a human sample is still expensive or even prohibitive for most labs. Very often investigators need to assay multiple samples to identify biologically interesting differences with reasonable statistical significance.

Additionally, bisulfite converted genomes have lower sequence complexity. This not only causes problems in library construction and cluster formation on a sequencing plate, but also more profoundly affects alignment of bisulfite reads to the genome, i.e. mapping. Several algorithms have been developed to improve mapping of WGBS data (Xi and Li 2009; Coarfa et al. 2010; Krueger and Andrews 2011; Frith et al. 2012; Otto et al. 2012), but the problem remains not entirely solved. The confidence of mapping WGBS reads is generally lower than mapping standard, non-bisulfite-converted reads. Since CpG methylation calls are predicted based on aligned reads, how accuracy of methylation calls relates to mapping quality remains uncharacterized. For example, while the effect of biased (C doesn't match T) versus non-biased (C matches T) alignment has been analyzed (Krueger et al. 2012), no one, to our knowledge, has examined the possibly more critical, alignment biases based on the number of Cs in a read in either type of alignment.

In contrast, MeDIP and MRE protocols produce standard sequencing reads for which existing statistics were designed. Although two libraries are constructed, the total cost (reagents and labor) is comparable to constructing one WGBS, according to published protocols (http://www.roadmapepigenomics.org/protocols). Mapping of MeDIP and MRE reads uses standard mapping tools and is more accurate than mapping of reads from WGBS.

In our experimental validation, we examined 13 loci where MethylC-seq and methylCRF predictions do not agree in H1 ESC. We used bisulfite conversion, PCR, cloning and

Downloaded from genome.cshlp.org on July 16, 2026 . Published by Cold Spring Harbor Laboratory Press

sequencing as our validation method because it is considered the gold-standard for targeted DNA methylation prediction, and we could exclude the possibility that differences are caused by bisulfite conversion. Nevertheless, in 11 out of 12 loci the gold-standard approach gave methylation levels that were closer to those from methylCRF predictions than from WGBS. Our interpretation of this result is that most errors made by WGBS might be due to misalignment, however a comprehensive analysis of WGBS mapping is needed to be certain. Alternatively, these differences may reflect true biological variation. This raises the profound question again – how much of the WGBS predicted DNA methylome is actually incorrect due to challenges in mapping bisulfite converted reads? We are eager to explore this question in future studies.

When compared to RRBS and Illumina arrays, our method is obviously much more comprehensive. Our method provides 10 to 20 fold more coverage than RRBS or available methylation arrays. Investigators may want to use array-based assays when their target CpG sites are directly interrogated by the array. However, many regions of interest, for example, repeats or cryptic promoters, will not be assessed. There are also a number of examples where the specific CpG site interrogated by an array does not reflect the true methylation status of the genomic feature (e.g. a promoter) and may lead to false conclusions. Our method not only provides a comprehensive method for exploratory studies, but as the cost of WGBS drops sufficiently for exploratory analysis, the concomitant drop in cost of methylCRF application on MeDIP-seq and MRE-seq will provide investigators a platform to comprehensively address biological questions by comparing multiple samples, conditions, or variances genome-wide.

The accuracy of methylCRF was benchmarked against WGBS, RRBS, Infinium array, and locus specific-bisufite sequencing on H1 human ESCs. In addition, we determined that the high concordance between methylCRF and WGBS is consistent across most genomic feature sets and across all CpG density levels. The power of the method stems from its integrative nature – methylCRF is able to integrate *a priori* information about the expected methylation states of various types of genomic features, two complementary and independent experimental measurements of methylation states, and hidden relationships among neighboring CpG sites. Genomic sequences and features provide a default expectation of their methylation status. Indeed, CpG content of the genome reflects germ cell methylation states during the course of evolution (Li et al. 2012) and has been used to estimate methylation levels directly (Das et al. 2006). This is reflected by the overall concordance of 0.66 when methylCRF makes predictions based on genomic features alone, which represents an expectation of methylation of a majority of CpGs in a normal somatic cell. The concordance is significantly improved when either MeDIP-seq or MRE-seq data are integrated, and the highest concordance is obtained when the

Downloaded from genome.cshlp.org on July 16, 2026 . Published by Cold Spring Harbor Laboratory Press

datasets are combined. Importantly, methylation predictions made by methylCRF are conditioned on both genomic features and experimental data, and not driven by genomic features alone. This is supported by the accurate separation of methylated CpG islands from unmethylated ones (**Fig. 6D**), even when focusing on promoter regions and/or intergenic CpG islands (**Supplementary Fig. 1, 2**).

The accuracy of methylCRF was further benchmarked on WGBS and Infinium array data from a second sample. Here methylCRF trained on H1 ESC data was applied to MeDIP-seq and MRE-seq of a fetal brain NSCs sample. The concordances between methylCRF and WGBS, and between methylCRF and Infinium array were at similarly high levels as those obtained on analyzing H1 ESC data. Moreover, methylCRF can reliably identify differentially methylated regions between the two samples. This strongly suggests that our model trained on ESC data can be applied to data of other samples.

In the current implementation of methylCRF we only consider CpG methylation and assume all signals obtained from MeDIP-seq and MRE-seq are results of CpG methylation. We also assume WGBS produced methylation signal and ignore complications caused by hydroxymethylation. We note that methylations of cytosines in the context of other than CpG (i.e., CHG and CHH) are rare in somatic cells but are indeed present in embryonic stem cells, usually in low levels and are associated with highly methylated CpGs (Lister et al. 2009). Biological significance of CHG and CHH methylation in mammalian cells is yet to be determined. Our statistical model is general enough to incorporate non-CpG cytosine methylation, but we focused on CpG methylation in this study. Our statistical model is also general enough to incorporate data on hydroxymethylation when they become more and more available.

Our study has several limitations. Because the cell line we used to train, H1 ESC, is male it is possible that the additional X chromosomes in female samples may not be as accurate. This is because males will only have one allele aligning the reference X chromosome whereas a female will have two, resulting in twice as many reads. In fact, this may also effect WGBS accuracy. The concordance within 0.25 difference window between H1 and H9 on chrX alone drops to 81% whereas excluding chrX raises the concordance 92%. The concordance of methylCRF with H9 on chrX is 79% whereas without it is 90%. Note that this also provides a natural experiment that suggests how methylCRF will perform in cases of large scale genomic aberrations such as segmental or even chromosomal duplication or deletion, which is frequently found in cancer. Both WGBS and methylCRF seem to be proportionally less accurate when alleles and possibly segments are added or deleted. Nevertheless, once more WBGS data becomes available, we can trivially extend methylCRF to include a field for structural variations

Downloaded from genome.cshlp.org on July 16, 2026 . Published by Cold Spring Harbor Laboratory Press

which could be estimated by standard means. Additionally, since MeDIP-seq and MRE-seq are sequencing based, we can make use of existing tools to add SNP-based features and to include input (un-enriched sequences). We note that WGBS is at a disadvantage when considering SNPs, in particular C->T SNP's will either be reported as an un-methylated C unless strand-specific alignment is available or even worse will align to cause false-positive alignments in other locations.

Another potential limitation is that the H1 WGBS (MethylC-seq) and MeDIP-seq and MRE-seq were performed on separate passages of the H1 ESC line and assayed in separate labs. This may explain why methylCRF was consistently validated by the bisulfate cloning method over WGBS. However, if this were true, two important inferences can be drawn. One, notable changes in methylation can be seen even between passage numbers. Two, these validations show methylCRF's sensitivity in detecting DMRs based on experimental data – even in very similar biological contexts. Additionally, the accuracy on fetal NSCs is slightly lower than on H1 ESC's. This may suggest that H1 ESC's may have differences in their global methylation than other cell types. While this does not stop methylCRF from detecting tissue-specific DMR's, it suggests that the accuracy may improve further if we re-train methylCRF simultaneously on WGBS from multiple cell-types.

Finally, because of our use of genomic feature-specific predictions, methylCRF accuracy may suffer when some part of the methylation machinery breaks down or behaves differently, for instance as in some cancers. We have indirectly tested this in a sample case, however. **Fig. 2C** shows CpG islands to have an extremely biased distribution of low methylation. However, **Fig. 6D** shows equivalent accuracy in CpG islands that represent a genomic feature with, in the statistical view of methylCRF, aberrant methylation.

Despite the promise of WGBS based methods, the number of publicly available, complete, single CpG resolution DNA methylomes is still small in contrast to the number of lower resolution and/or lower coverage DNA methylomes generated by less expensive methods (e.g., MeDIP-seq and MRE-seq generated by individual labs and by the Roadmap Epigenomics project). Our method can convert these data into single base resolution, complete DNA methylomes, thus significantly increase the value of such existing datasets.

In summary, our results suggest that methylCRF is an effective statistical framework capable of integrating two fundamentally different sequencing-based DNA methylation assays, MeDIP-seq and MRE-seq, to predict genome-wide, single CpG resolution methylome maps. The concordance of our methylCRF predictions with WGBS falls within the range of concordance between two WGBS experiments on similar cells. methylCRF will thus significantly increase the

Downloaded from genome.cshlp.org on July 16, 2026 . Published by Cold Spring Harbor Laboratory Press

value of high-coverage DNA methylomes produced using much less expensive methods, and provide a general statistical framework for integrating contributions from various types of DNA methylation data regardless of their coverage, resolution, and nature of their readout.

METHODS

methylCRF implementation

methylCRF is implemented using the theoretical framework of conditional random fields (Lafferty et al. 2001). This general framework expresses the conditional probability Pr(Y|X) of a series of hidden states, the random variables, Y, given observed data X:

$$P(\boldsymbol{Y}|\boldsymbol{X}) = \frac{1}{Z}\prod_{c=1}^{C} e^{\sum_{k=1}^{K} w_k * f_k(c, y_{c-1}, y_c, \boldsymbol{X})} \quad where$$

Y is the methylation level of every CpG; X is the observations (MeDIP-seq, MRE-seq, genomic context). The *C* CpGs are indexed by *c*, and the *K* feature functions, *f*, are indexed by *k*. The weights, w_1 .. w_k, are learned via gradient ascent of the log likelihood. Z is the partition function which provides the global normalization and is the sum of all sequences of methylation levels given X:

$$Z = \sum_{y \epsilon Y} \prod_{c=1}^{C} e^{\sum_{k=1}^{K} w_k * f_k(c, y_{c-1}, y_c, \boldsymbol{X})}$$

Our approach to data features was to initially include anything that we thought might in some way effect methylation. We then let an L1 normalization term during training determine which features were not important by pushing their weights to 0. Therefore, the choice of important features was learned from the data. We split the data into different ranges of effect. We included MeDIP and MRE scores both at the CpG (D0 and M0) and within windows of 20bp, 200bp, 2kbp, and 20kbp windows. We included whether a CpG was at an MRE restriction site (ER) and the distance in bp to the previous CpG (PC). From UCSC genome browser tracks (Kent et al. 2002) we included a 46-way mammalian phastCons conservation score. We included GC% in 20bp, 150bp, and 500bp windows, and CpG density in a 150bp window.

We defined one CRF feature for each one of these data features combined with the methylation level of the current and previous, 5', CpG. We also added CRF features for the next two MeDIP and MRE scores on both the 5' and 3' sides. We then defined compound features.

Downloaded from genome.cshlp.org on July 16, 2026 . Published by Cold Spring Harbor Laboratory Press

We included a feature combining D0 and PC to possibly address the nonlinear relationship between MeDIP and CpG density. We also included one large feature including factors that appeared to be interacting (data not shown) including both the current and previous CpG methylation as well as D0, M0, and PC for the current CpG as well as the two CpGs to the upstream and downstream of the current. This feature also included MeDIP and MRE in 20bp and 2kbp windows, ER, and GC in 20bp and 150bp windows for the current CpG as well as ER for the surrounding two CpG's. We additionally included four more features consisting of subsets of these as a fallback for rare combinations of values. A diagram of the complete model is illustrated in **Supplementary Fig. S5**.

The distributions of methylation levels are genomic feature-specific (**Fig. 2C**), so we reasoned that the methylation level transitions between neighboring CpGs are also genomic feature-specific. To address this, we trained a separate CRF for each genomic feature: one for each of the genomic annotations in RefGene (5' UTR, gene body, exon, intron, 3'UTR, CGI), for the derived types (distal promoter, TSS-2kb; proximal promoter, TSS-250bp; core promoter, TSS +/- 35bp; 1kbp flanking each CpG Island; and 2kbp flanking each CpG Island), one for each Repeat class (DNA, LINE, LTR, RNA, SINE, low complexity sequence and simple repeats, and other), and one for the remainder of the genome not covered by any of the previous CRFs.

Training was performed using MethylC-seq (Lister et al. 2009) measured methylation levels in randomly chosen regions representing 20% of the genome. We used only CpGs with at least 10-read coverage. We performed separate discretization for each CRF. Each of the CRFs were trained using crfsgd (Bottou and Bousquet 2008) using default settings.

CRFs are typically discriminately trained by iteratively ascending their gradient. While the function is convex and so converges to a global maximum, the whole CRF must be evaluated once for every iteration in the ascent which poses performance issues. However, CRFs have been shown to handily model millions of features (Sha and Pereira 2003). Additionally, the ascent can be performed online providing two benefits: 1) potentially less over-fitting due to the less optimal solution, and 2) speed of analysis (Bottou and Bousquet 2008). Being discriminately trained, though, CRFs need to be handled carefully so as to ensure their generalizability to future data.

For CpG's that are annotated with multiple features, we combine the methylation predictions by averaging the predictions of the corresponding CRF's and giving each CRF an equal vote. Performance was evaluated using CpGs that were not used for training.

Downloaded from genome.cshlp.org on July 16, 2026 . Published by Cold Spring Harbor Laboratory Press

Discretization Heuristic

CRFs are rooted in the Natural Language Processing (NLP) community and so model discrete rather than continuous variables. There has been at least one paper extending CRFs to rankings which requires developing a continuous CRF (Qin et al. 2008). Additionally, in the derivation of CRFs there is no restriction on the form of the random variables, so continuous predictors are also an option. However, the theoretical and practical work on modeling and training of discrete CRFs is very extensive. Additionally, the relationship between the predictors and the methylation ratios are complex. Finally, Naïve Bayes is known to perform better with discretized variables (Dougherty et al. 1995). We, therefore, decided to follow in this line of work by representing the relationship between the predictors and methylation ratios as piece-wise constant. The trade-off in avoiding the choice of the correct family of continuous distributions for the methylation ratios as well as the predictors in the continuous case, is that we must determine where to cut the range of a predictor into pieces. This is equivalent to discretization for which considerable work has been done.

While equal range or equal size discretization is straightforward, they did not perform very well (data not shown). We instead chose to use supervised discretization using the methylation ratios to guide the discretization. While good entropy-based methods do exist, they would require the methylation ratios to already be discretized posing a chicken and the egg problem for which we could not find an existing solution. This lead us to develop a 2-step heuristic consisting of clustering to discretize the methylation ratios followed by supervised discretization of each predictor. In the first step, which we term “order-preserving clustering”, we cluster the predictors and the methylation ratios together. We iteratively up-weight the methylation ratios and re-cluster until there is an order between clusters such that all of the methylation values in one cluster are larger than the previous (**Supplementary Fig. 6**). Given this as a data model-driven discretization of the methylation ratios, we then use supervised discretization on each predictor individually. Note that this heuristic can use any pair-wise distance metric, clustering method, or supervised discretization method. We used k-means (Macqueen 1967) and Euclidean distance for clustering and CAIM (Kurgan and Cios 2004) for discretization.

MeDIP-seq, MRE-seq, and WGBS data

All data were obtained from the NIH Roadmap Epigenomics Mapping Centers’ repository for human reference epigenome atlas (Bernstein et al. 2010). Experiments were performed under the guidelines of the Roadmap Epigenomics project (http://www.roadmapepigenomics.org/protocols). Specifically, MeDIP-seq and MRE-seq

Downloaded from genome.cshlp.org on July 16, 2026 . Published by Cold Spring Harbor Laboratory Press

experiments were performed as described previously (Maunakea et al. 2010). All data have been previously submitted to NCBI, and are listed in **Supplementary Table 1**.

The reads were aligned with bowtie (Langmead et al. 2009) to HG19. The MRE reads were normalized to account for differences in enzyme efficiency and scoring consisted of tabulating reads with ends at each CpG (Maunakea et al. 2010). To allow for comparison between experiments, the CpG read counts for MeDIP were scaled so that the 75th percentile of CpGs with at least one read is 10. Since for each MeDIP read, the CpG that was bound by the antibody cannot be determined, a fractional count was added to each CpG for the read. The final MeDIP score is the sum of CpG scores within the specified window.

Genomic features

RepeatMasker annotations, CpG islands, genomic super duplications, 46-way phastCons, and refGene coding loci features were all downloaded from UCSC Genome Browser (Kent et al. 2002). The GC percent, CpG density, and MRE sites were calculated using HG19.

Training and prediction

For training, we randomly selected both the location and size of genomic fragments of 75kb to 750kb in length comprising roughly 20% of the genome. We used only CpGs with at least 10 BS reads. We performed separate discretization for each CRF. For the k-means step in the discretization of BS methylation values, we arbitrarily chose 10 clusters as this seemed a reasonable cutoff for the granularity for the measurement of CpG methylation that we would be interested in. We used Euclidean distance as our metric. Further details on our discretization method are discussed above. Each of the CRFs were trained using crfsgd (Bottou and Bousquet 2008) using default settings. The data for each CRF was split on gaps of greater than 750bp between consecutive CpG's.

For prediction, the data was created as for the training data. For the final methylCRF predictions, we combined the predicted methylation levels of all the CRFs by averaging the predictions for CpGs that were shared by multiple CRFs.

Genome Browser tracks are available as part of Roadmap Epigenomics Project's data visualization hub:

http://VizHub.wustl.edu

Bisulfite treatment and library construction for WGBS

Downloaded from genome.cshlp.org on July 16, 2026 . Published by Cold Spring Harbor Laboratory Press

1 to 5ug gDNA was sonicated to an approximate size range of 200-400bp. Size selection is performed on a PAGE gel to obtain DNA fragments of 200-300bp. DNA are quantified by fluorescent incorporation (Qubit, Invitrogen). The library preparation includes end-repair and phosphorylation with NEBNextTM or Illumina Sample Prep Kit reagents, and addition of an 'A' base to the 3' end of the DNA fragments. Methylated adapters are ligated and size selection is performed to remove excess free adaptors. The ligated DNA is quantified by Qubit, and approximately 100ng DNA is used for bisulfite conversion. Methylated-adaptor ligated to unmethylated lambda-phage DNA (NEB) is used as internal control for assessing rate of bisulfite conversion. The ratio of target library to Lambda is 1600:1. Bisulfite conversion of the methylated adapter-ligated DNA fragments follows the FFPE Tissue Samples Protocol from Qiagen's Epitect Bisulfite Kit. Cleanup of the bisulfite converted DNA is performed, and a 2nd round of conversion is applied. Enrichment of adaptor-ligated DNA fragments is accomplished by dividing the template into 5 aliquots followed by 8 cycles PCR with adaptor primers. Post PCR size-selection of the PCR products from the 5 reactions is performed on a PAGE gel. Following 100bp paired-end sequencing on a HiSeq2000, sequence reads were aligned and processed through the Bismark pipeline.

Infinium assay

Bisulfite conversion was performed on 1 ug of genomic DNA using the EZ DNA methylation kit (Zymo research) as per the manufacturer's alternative incubation conditions protocol. The bisulfite converted DNA was amplified and hybridized to an Infinium HumanMethylation450 beadchip (Illumina) following the Infinium HD methylation assay protocol at the UCSF Genomics Core facility. Methylation levels (beta values) were determined using the Methylation Module of the Illumina GenomeStudio software.

Bisulfite validation

Total genomic DNA underwent bisulfite conversion following an established protocol[10] with the following modifications: incubation at 95 °C for 1 min, 50 °C for 59 min for a total of 16 cycles. Regions of interest were amplified with PCR primers (**Table 1**) and subsequently cloned using pCR2.1/TOPO (Invitrogen). Individual bacterial colonies were subjected to PCR using vector-specific primers and sequenced (Quintara biosciences). The data were analyzed with online software BISMA (Rohde et al. 2010). Results are summarized in **Table 1** and **Supplementary Fig. 3**.

Downloaded from genome.cshlp.org on July 16, 2026 . Published by Cold Spring Harbor Laboratory Press

SOFTWARE AVAILABILITY

MethylCRF is complete open source software. The source code, parameter sets, genomic data sets, as well as instructions are available at:

http://methylCRF.wustl.edu

ACKNOWLEDGEMENT

We thank collaborators in the Reference Epigenome Mapping Centers (REMC), Epigenome Data Analysis and Coordination Center and NCBI who have generated and processed data used in this project. We acknowledge support from the NIH Roadmap Epigenomics Program, sponsored by the National Institute on Drug Abuse (NIDA) and the National Institute of Environmental Health Sciences (NIEHS). J.B.C is supported by a Career Development Award from the Dermatology Foundation. J.F.C., M.H. and T.W. are supported by NIH grant 5U01ES017154. T.W. is supported in part by the March of Dimes Foundation, the Edward Jr. Mallinckrodt Foundation, P50CA134254 and a generous start up package from Department of Genetics, Washington University. K.L.L. and C.L.M. are supported by NIH Grants P01CA095616 and P01CA142536 and a grant from the Sontag Foundation. T.W. thanks David Haussler for insightful discussions during the early development of the project.

DISCLOSURE DECLARATION

None declared.

TABLES

Table 1. Summary of validation results. Validation of 12 targets chosen within windows where there is discordance between MethylC-seq and methylCRF for H1 ESC. The root-mean-squared error (RMSE) is shown between MethylC-seq or methylCRF and bisulfite validation using the listed primers.

Fig. Panel	Tested Coordinates (hg19)	Fwd Primer	Rev Primer	MethylC-seq RMSE	methylCRF RMSE
S2A.	chr2 + 233216826 233217069	TTTTTTTAGAATTTAAATTTGGGTGAA	ATCCTACCTTAAATAAACACCTACC	0.28	**0.12**
S2B.	chr1 + 146551336	TTTTTTTTGGTTGAGGTTAGTTTAT	CCCAAACTCTAAATCAAAACTTTTT	0.16	**0.13**

Downloaded from genome.cshlp.org on July 16, 2026 . Published by Cold Spring Harbor Laboratory Press

	146551644				
S2C.	chr2 + 37571975 37572244	TAGTTTGGTTAGAG GAGAAGGTGAG	AACCCAAAAAAAA CCAATAACATC	0.52	**0.06**
S2D.	chr10 + 94820761 94821132	TTAGGAGTTAGGAA AAAGTTTTGAG	ACTAAACCAAACT AAACAACAAACC	0.44	**0.11**
S2E.	chr15 + 57025677 57025990	TGATTGGAGTTTTG AGGAGGA	CCCACATAAAAAC AAAACCCTAAC	0.46	**0.19**
S2F.	chr1 + 200343036 200343274	GGAGGGGAAGAAT ATAAGAAATAATTAG T	TCTAAATCCCAAT CCCTAACTACAA	**0.06**	0.82
S2G.	chr2 + 228736110 228736500	ATGTAGTTTAGGTT GTGGTTTAGGT	CAATCTAAAAACC CAAAATCCC	0.31	**0.05**
S2H.	chr4 + 103940626 103940995	TTAAGAATTTTATTG AATTGAGGGG	TAAACAAAAAACA CACCAAACAATC	0.20	**0.04**
8A.	chr22 + 19929336 19929659	GTTTTTGGGGTAG TTAGGGTTGT	CTCAACTTTCCAC AAAAAATCTAAAA	0.40	**0.12**
S2I.	chrX + 48929750 48930067	GTAGGTAGGTTAAT GGAGTGGTGAG	ACCAAAAAAACAA CCAAAACATACT	0.77	**0.03**
S2J.	chr13 + 58208240 58208505	TTTATATTTATGTG TTTGTGAATTTTA	ATACTCACCAAA TAACCCAAACC	0.53	**0.32**
8B.	chr19 + 35068305 35068683	TTTTGGTTAGAAATT GGTTAATGAT	CTAAAATACCACA AACCCCACTAC	0.50	**0.05**

FIGURE LEGENDS

Figure 1: Relationship between MeDIP-seq and MRE-seq and MethylC-seq. (**A**) A kernelized density plot of per CpG MeDIP-seq normalized read count values as a function of MethylC-seq methylation levels shows a complex, approximately proportional relationship. (**B**) MRE-seq normalized read counts as a function of MethylC-seq methylation levels shows a complex, approximately inversely proportional relationship.

Figure 2. CpG methylation levels are non-random throughout the genome. (**A**) A kernelized density plot of MethylC-seq methylation levels as a function of CpG density. Methylation varies in a CpG density dependent manner with the majority of CpGs at 0-0.75 density with 75%-100%

Downloaded from genome.cshlp.org on July 16, 2026 . Published by Cold Spring Harbor Laboratory Press

methylation and a smaller group at 0.75-1.25 density with almost 0% methylation. (**B**) CpG methylation levels as a function of their immediately 5' CpG methylation level (up to 750bp). (**C**) Distribution of MethylC-seq methylation levels at CpG islands, exons, and introns.

Figure 3: CRF versus HMM. (**A**) In a HMM, the labels generate the observations, while in a CRF co-occurrences of the label and observations are associated. (**B**) HMMs model the joint probability and must consequently model the dependencies in the observations, while CRFs only model the dependencies of the label on the data.

Figure 4: Concordance Between MethylC-seq and methylCRF. (A) Kernelized density plot comparing H1 ESC (male) MethylC-seq and methylCRF methylation levels at each CpG with at least 1 MethylC-seq read. MethylCRF recapitulates the bi-modal distribution of MethylC-seq. **(B)** The number of CpGs as a function of the difference between MethylC-seq and methylCRF methylation levels – the two agree within 25% for 91% of the CpGs and within 10% for 70% of the CpGs. The difference between BS-seq (H9 ESC, female) and MethylC-seq (H1 ESC) on common CpGs is also plotted for comparison. **(C)** Genome Browser view of per CpG methylation levels across a representative test region on chromosome 1.

Figure 5: Comparison between MethylC-seq and methylCRF and other methylation assays. (A) Concordance of methylCRF, BS-seq, RRBS, and Infinium array with MethylC-seq within a 25% window broken out by annotated genomic features. Note that BS-seq (H9) is a female sample, while MethylC-seq (H1) is a male sample. Only CpG's in common were compared. (**B**) The number of CpGs used for each comparison on a log10 scale.

Figure 6: Factors Affecting Concordance Between MethylC-seq and methylCRF. (A) Concordance with MethylC-seq as a function of MethylC-seq read count (CpG coverage) at 10% and 25% windows for both methylCRF and BS-seq. The right y-axis (blue bars) indicates the number of CpGs with that coverage. **(B)** Concordance with MethylC-seq as a function of CpG density at 25% windows for both methylCRF and BS-seq. **(C)** Concordance of methylCRF within a 25% window broken out by annotated genomic features when only MeDIP-seq, MRE-seq, or genomic features are used. Concordance of BATMAN using MeDIP-seq is also plotted for comparison. **(D)** methylCRF accuracy on CGIs with high or low methylation (as defined by MethylC-seq). The Lo set of CGIs are those with an average CpG methylation <= 0.2, while the Hi set are those with an average methylation >= 0.8.

Downloaded from genome.cshlp.org on July 16, 2026 . Published by Cold Spring Harbor Laboratory Press

Figure 7: Applying methylCRF to fetal NSCs. (A) Concordances between methylCRF and WGBS data and between methylCRF and Infinium array broken out by annotated genomic features. **(B)** CpG islands were grouped as “indifferent” and “different” based on their methylation levels in H1 ESC and fetal NSC (Hu-F-NSC-02) assessed by WGBS data. Actual difference distributions were plotted between H1 ESC (WGBS, red), or H9 ESC (WGBS, blue), or H1 ESC (methylCRF, green) and fetal NSCs (WGBS).

Figure 8: Comparing methylCRF and WGBS predictions in imprinted control regions. (A) Known imprinted control regions (ICRs, https://atlas.genetics.kcl.ac.uk, **Supplementary Table 2**) were grouped based on WGBS data (H1 ESC, MethylC-seq), as “Lo” (average methylation <=0.2), “Mid” (average methylation between 0.2 and 0.8), and “Hi” (average methylation >=0.8). Boxplots represent average methylation levels of these ICRs based on MethylC-seq and methylCRF. **(B)** Same as **(A)**, except for fetal NSCs. **(C)** A genome browser view of ICR near gene MEST (mesoderm specific transcript, chr7). **(D)** A genome browser view of ICR near gene NDN (necdin, chr15).

Figure 9: Experimental validation of regions where there is discordance between MethylC-seq and methylCRF. Genome browser view and site-specific bisulfite sequencing validation for each region (open circle: unmethylated CpG; filled circle: methylated CpG). The line graph shows the methylation levels estimated by MethylC-seq, RRBS, bisulfite validation, and methylCRF. (**A**) chr22:19929336-19929659; MethylC-seq predicted on average a methylation level of 80% methylated, while methylCRF and bisulfite validation agreed on a level of 40% methylated. **(B)** chr19: 35068305-35068683; MethylC-seq predicted on average a methylation level of 60% methylated, while methylCRF and bisulfite validation agreed that the region is more than 90% to completely methylated.

REFERENCES:

Bernstein BE, Stamatoyannopoulos JA, Costello JF, Ren B, Milosavljevic A, Meissner A, Kellis M, Marra MA, Beaudet AL, Ecker JR et al. 2010. The NIH Roadmap Epigenomics Mapping Consortium. *Nat Biotechnol* **28**(10): 1045-1048.

Bock C. 2012. Analysing and interpreting DNA methylation data. *Nature reviews Genetics* **13**(10): 705-719.

Downloaded from genome.cshlp.org on July 16, 2026 . Published by Cold Spring Harbor Laboratory Press

Bock C, Tomazou EM, Brinkman AB, Muller F, Simmer F, Gu H, Jager N, Gnirke A, Stunnenberg HG, Meissner A. 2010. Quantitative comparison of genome-wide DNA methylation mapping technologies. *Nat Biotechnol* **28**(10): 1106-1114.

Bottou L, Bousquet O. 2008. The tradeoffs of large scale learning. *Advances in neural information processing systems* **20**: 161-168.

Chavez L, Jozefczuk J, Grimm C, Dietrich J, Timmermann B, Lehrach H, Herwig R, Adjaye J. 2010. Computational analysis of genome-wide DNA methylation during the differentiation of human embryonic stem cells along the endodermal lineage. *Genome Res* **20**(10): 1441-1450.

Coarfa C, Yu F, Miller C, Chen Z, Harris R, Milosavljevic A. 2010. Pash 3.0: A versatile software package for read mapping and integrative analysis of genomic and epigenomic variation using massively parallel DNA sequencing. *BMC Bioinformatics* **11**: 572.

Cokus SJ, Feng S, Zhang X, Chen Z, Merriman B, Haudenschild CD, Pradhan S, Nelson SF, Pellegrini M, Jacobsen SE. 2008. Shotgun bisulphite sequencing of the Arabidopsis genome reveals DNA methylation patterning. *Nature* **452**(7184): 215-219.

Das R, Dimitrova N, Xuan Z, Rollins RA, Haghighi F, Edwards JR, Ju J, Bestor TH, Zhang MQ. 2006. Computational prediction of methylation status in human genomic sequences. *Proc Natl Acad Sci U S A* **103**(28): 10713-10716.

DeCaprio D, Vinson JP, Pearson MD, Montgomery P, Doherty M, Galagan JE. 2007. Conrad: gene prediction using conditional random fields. *Genome Res* **17**(9): 1389-1398.

Dougherty J, Kohavi R, Sahami M. 1995. Supervised and unsupervised discretization of continuous features. *MACHINE LEARNING-INTERNATIONAL WORKSHOP THEN CONFERENCE*(194-202).

Down TA, Rakyan VK, Turner DJ, Flicek P, Li H, Kulesha E, Graf S, Johnson N, Herrero J, Tomazou EM et al. 2008. A Bayesian deconvolution strategy for immunoprecipitation-based DNA methylome analysis. *Nature biotechnology* **26**(7): 779-785.

Frith MC, Mori R, Asai K. 2012. A mostly traditional approach improves alignment of bisulfite-converted DNA. *Nucleic Acids Res* **40**(13): 28.

Harris RA, Wang T, Coarfa C, Nagarajan RP, Hong C, Downey SL, Johnson BE, Fouse SD, Delaney A, Zhao Y et al. 2010. Comparison of sequencing-based methods to profile DNA methylation and identification of monoallelic epigenetic modifications. *Nat Biotechnol* **28**(10): 1097-1105.

Jones PA. 2012. Functions of DNA methylation: islands, start sites, gene bodies and beyond. *Nat Rev Genet* **13**(7): 484-492.

Kent WJ, Sugnet CW, Furey TS, Roskin KM, Pringle TH, Zahler AM, Haussler D. 2002. The human genome browser at UCSC. *Genome Res* **12**(6): 996-1006.

Krueger F, Andrews SR. 2011. Bismark: a flexible aligner and methylation caller for Bisulfite-Seq applications. *Bioinformatics* **27**(11): 1571-1572.

Krueger F, Kreck B, Franke A, Andrews SR. 2012. DNA methylome analysis using short bisulfite sequencing data. *Nat Methods* **9**(2): 145-151.

Kurgan LA, Cios KJ. 2004. CAIM discretization algorithm. *IEEE Trans on Knowl and Data Eng* **16**(2): 145-153.

Lafferty J, McCallum A, Pereira F. 2001. Conditional Random Fields: Probabilistic Models for Segmenting and Labeling Sequence Data. *Departmental Papers* **CIS-159**.

Laird PW. 2010. Principles and challenges of genomewide DNA methylation analysis. *Nature reviews Genetics* **11**(3): 191-203.

Langmead B, Trapnell C, Pop M, Salzberg SL. 2009. Ultrafast and memory-efficient alignment of short DNA sequences to the human genome. *Genome Biol* **10**(3): R25.

Laurent L, Wong E, Li G, Huynh T, Tsirigos A, Ong CT, Low HM, Kin Sung KW, Rigoutsos I, Loring J et al. 2010. Dynamic changes in the human methylome during differentiation. *Genome Res* **20**(3): 320-331.

Downloaded from genome.cshlp.org on July 16, 2026 . Published by Cold Spring Harbor Laboratory Press

Li J, Harris RA, Cheung SW, Coarfa C, Jeong M, Goodell MA, White LD, Patel A, Kang S-H, Shaw C et al. 2012. Genomic hypomethylation in the human germline associates with selective structural mutability in the human genome. *PLoS Genet* **8**(5): 17.

Lister R, Pelizzola M, Dowen RH, Hawkins RD, Hon G, Tonti-Filippini J, Nery JR, Lee L, Ye Z, Ngo QM et al. 2009. Human DNA methylomes at base resolution show widespread epigenomic differences. *Nature* **462**(7271).

Macqueen J. 1967. Some methods of classification and analysis of multivariate observations. *Proceedings of the Fifth Berkeley Symposium on Mathematical Statistics and Probability*.

Maunakea AK, Nagarajan RP, Bilenky M, Ballinger TJ, D'Souza C, Fouse SD, Johnson BE, Hong C, Nielsen C, Zhao Y et al. 2010. Conserved role of intragenic DNA methylation in regulating alternative promoters. *Nature* **466**(7303): 253-257.

Meissner A, Mikkelsen TS, Gu H, Wernig M, Hanna J, Sivachenko A, Zhang X, Bernstein BE, Nusbaum C, Jaffe DB et al. 2008. Genome-scale DNA methylation maps of pluripotent and differentiated cells. *Nature* **454**(7205): 766-770.

Nair SS, Coolen MW, Stirzaker C, Song JZ, Statham AL, Strbenac D, Robinson MD, Clark SJ. 2011. Comparison of methyl-DNA immunoprecipitation (MeDIP) and methyl-CpG binding domain (MBD) protein capture for genome-wide DNA methylation analysis reveal CpG sequence coverage bias. *Epigenetics* **6**(1): 34-44.

Otto C, Stadler P, Hoffmann S. 2012. Fast and sensitive mapping of bisulfite-treated sequencing data. *Bioinformatics* **28**(13): 1698-1704.

Pelizzola M, Koga Y, Urban AE, Krauthammer M, Weissman S, Halaban R, Molinaro AM. 2008. MEDME: an experimental and analytical methodology for the estimation of DNA methylation levels based on microarray derived MeDIP-enrichment. *Genome Res* **18**(10): 1652-1659.

Qin T, Liu T, Zhang X, Wang D, Li D, Koller D, Schuurmans D, Bengio Y, Bottou L. 2008. Global ranking using continuous conditional random fields. *NIPS*.

R. Durbin SRE, A. Krogh, G. J. Mitchison. 1998. Biological Sequence Analysis: Probabilistic Models of Proteins and Nucleic Acids. *Cambridge University Press*.

Robertson KD. 2005. DNA methylation and human disease. *Nature reviews Genetics* **6**(8): 597-610.

Rohde C, Zhang Y, Reinhardt R, Jeltsch A. 2010. BISMA--fast and accurate bisulfite sequencing data analysis of individual clones from unique and repetitive sequences. *BMC Bioinformatics* **11**(230): 230.

Serre D, Lee BH, Ting AH. 2009. MBD-isolated Genome Sequencing provides a high-throughput and comprehensive survey of DNA methylation in the human genome. *Nucleic acids research* **38**(2): 391-399.

Sha F, Pereira F. 2003. Shallow parsing with conditional random fields. 213-220.

Suzuki MM, Bird A. 2008. DNA methylation landscapes: provocative insights from epigenomics. *Nature reviews Genetics* **9**(6): 465-476.

Wallach H. 2004. Conditional Random Fields: An Introduction. *Technical Report MS-CIS-04-21 Department of Computer and Information Science, University of Pennsylvania*.

Weber M, Davies JJ, Wittig D, Oakeley EJ, Haase M, Lam WL, Schubeler D. 2005. Chromosome-wide and promoter-specific analyses identify sites of differential DNA methylation in normal and transformed human cells. *Nat Genet* **37**(8): 853-862.

Xi Y, Li W. 2009. BSMAP: whole genome bisulfite sequence MAPping program. *BMC Bioinformatics* **10**: 232.

Yin X, Li J. 2010. Detecting copy number variations from array CGH data based on a conditional random field model. *J Bioinform Comput Biol* **8**(2): 295-314.

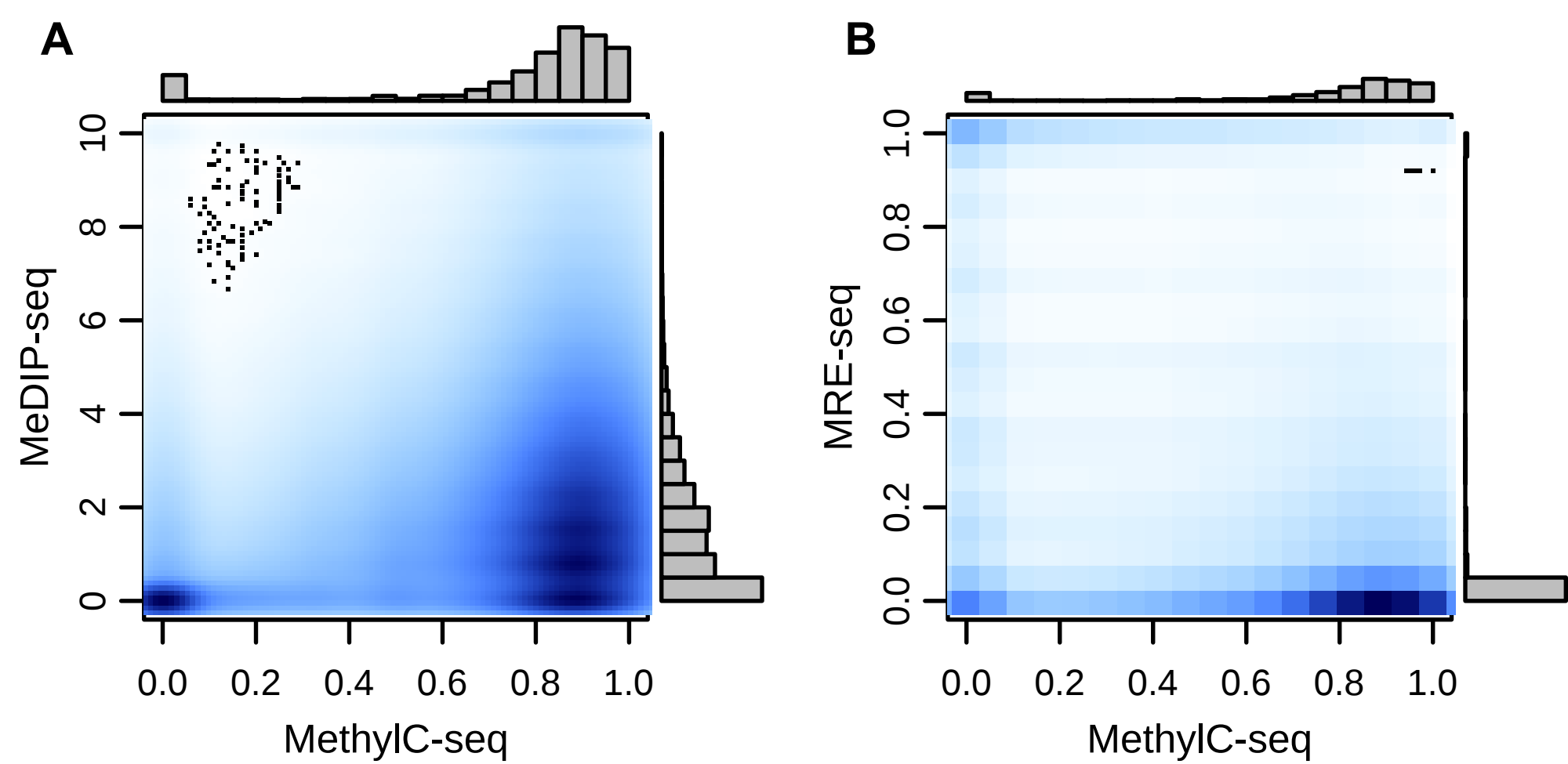
A
MeDIP-seq
0
2
4
6
8
10
0.0
0.2
0.4
0.6
0.8
1.0
MethylC-seq
B
MRE-seq
0.0
0.2
0.4
0.6
0.8
1.0
0.0
0.2
0.4
0.6
0.8
1.0
MethylC-seq

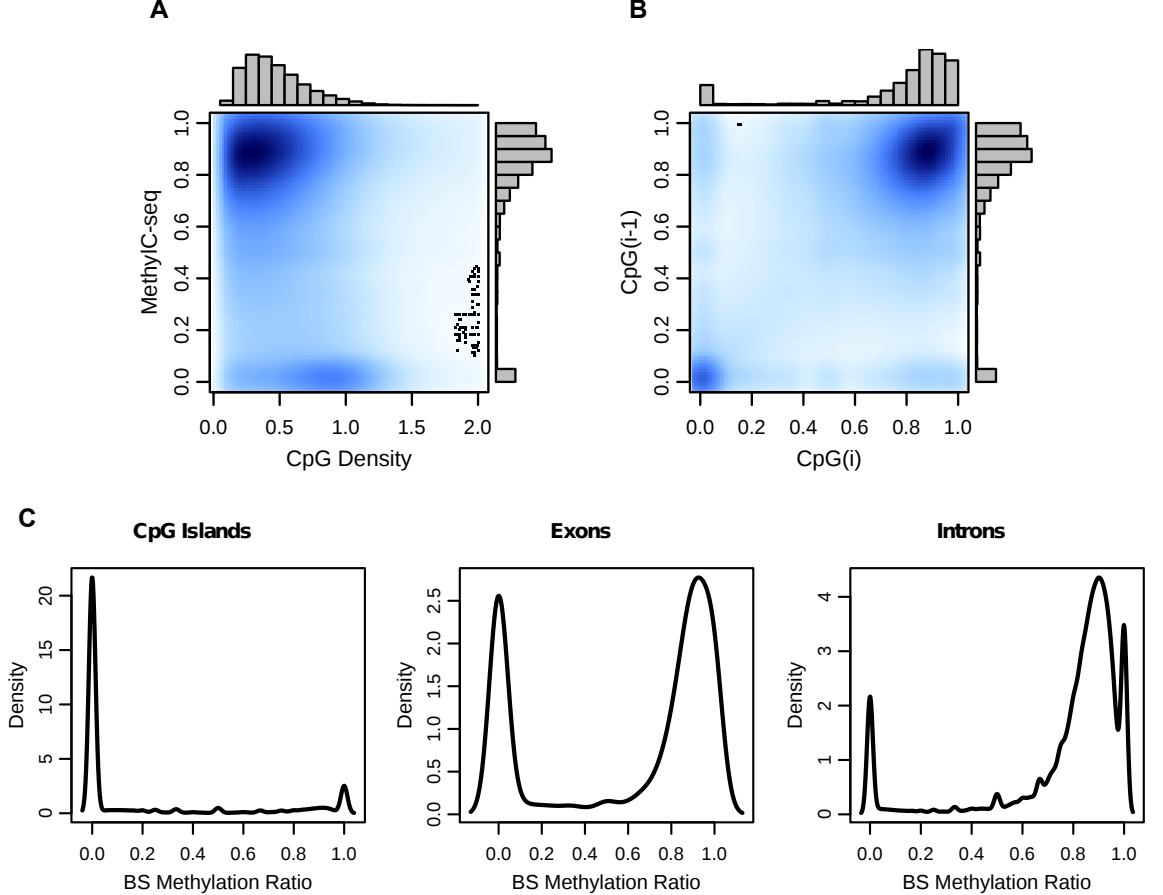
A
MethylC-seq
CpG Density
B
CpG(i-1)
CpG(i)
C
CpG Islands
Exons
Introns
Density
BS Methylation Ratio

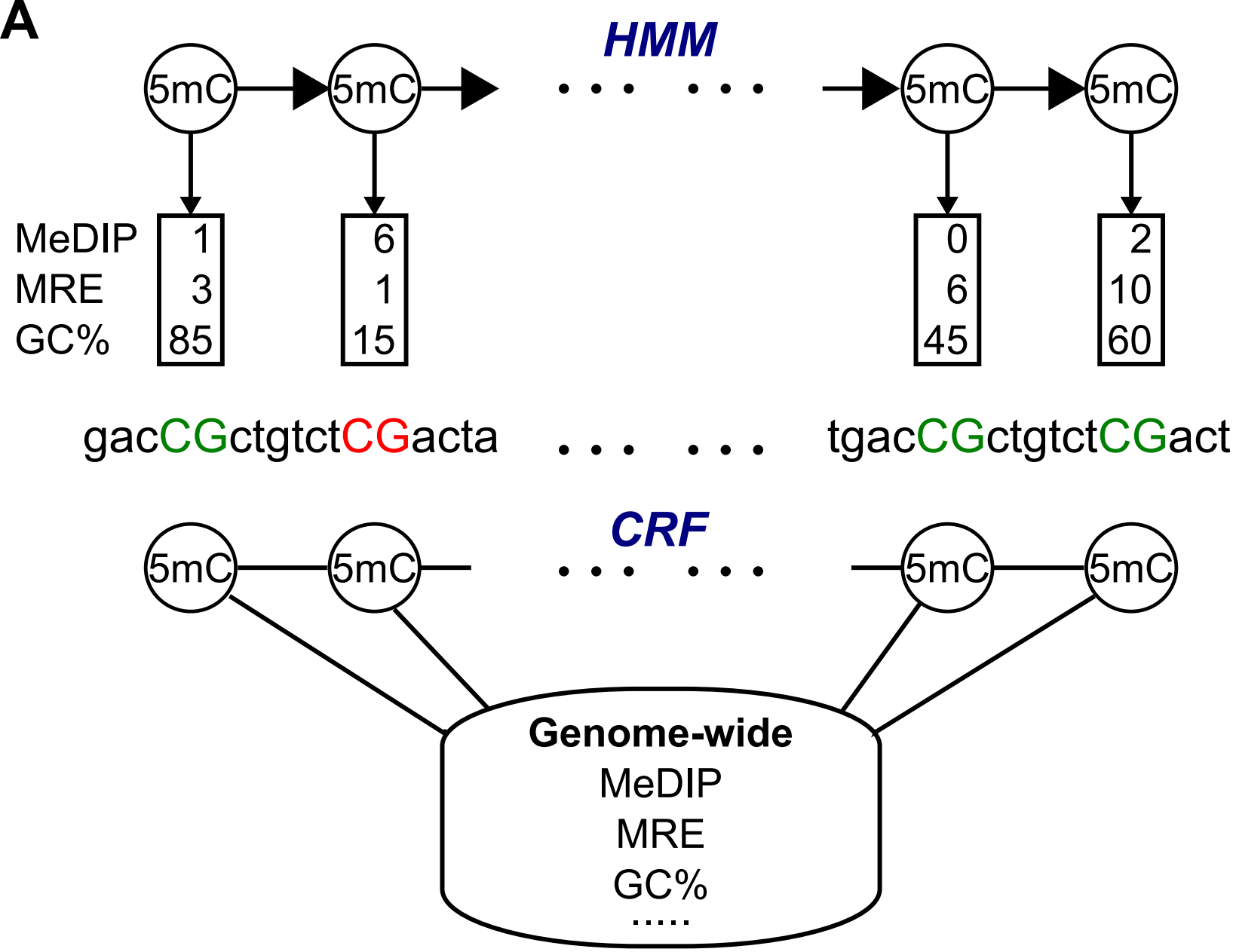

B

$$HMM := P(5mC)P(MeDIP, MRE, ... \mid 5mC)$$
$$= P(5mC, MeDIP, MRE, ...)$$
$$= P(5mC \mid MeDIP, MRE, ...)P(MeDIP, MRE, ...)$$

$$CRF := P(5mC \mid MeDIP, MRE, ...)$$

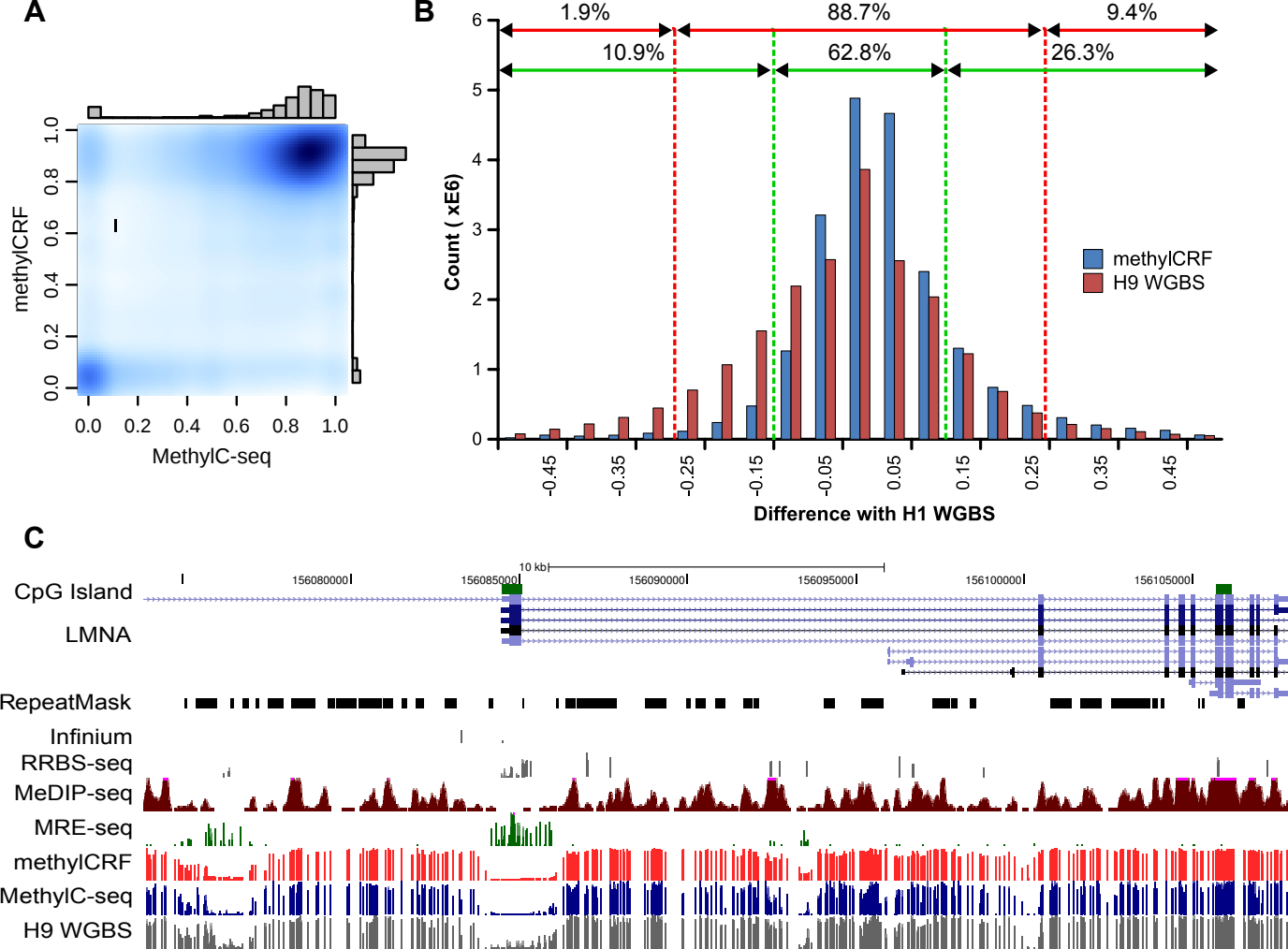
A
methylCRF
MethylC-seq
0.0
0.2
0.4
0.6
0.8
1.0
B
1.9%
88.7%
9.4%
10.9%
62.8%
26.3%
Count (xE6)
methylCRF
H9 WGBS
Difference with H1 WGBS
-0.45
-0.35
-0.25
-0.15
-0.05
0.05
0.15
0.25
0.35
0.45
C
10 kb
156080000
156085000
156090000
156095000
156100000
156105000
CpG Island
LMNA
RepeatMask
Infinium
RRBS-seq
MeDIP-seq
MRE-seq
methylCRF
MethylC-seq
H9 WGBS

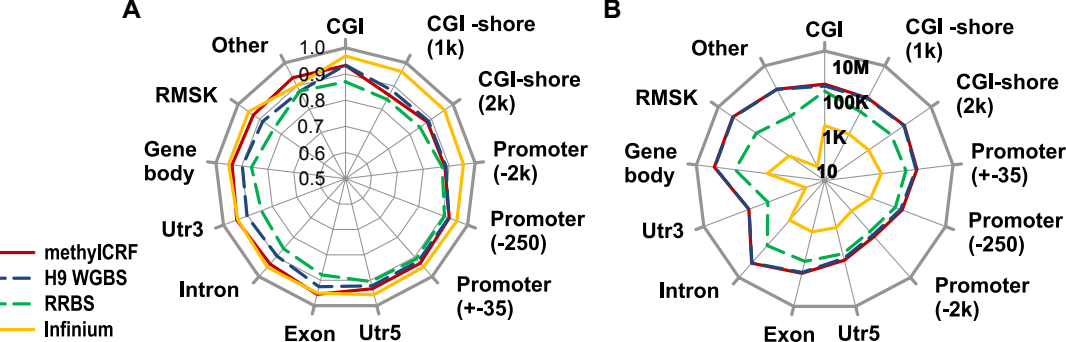
A
CGI
CGI -shore (1k)
CGI-shore (2k)
Promoter (-2k)
Promoter (-250)
Promoter (+-35)
Exon
Utr5
Intron
Utr3
Gene body
RMSK
Other
1.0
0.9
0.8
0.7
0.6
0.5
methylCRF
H9 WGBS
RRBS
Infinium
B
CGI
CGI -shore (1k)
CGI-shore (2k)
Promoter (+-35)
Promoter (-250)
Promoter (-2k)
Exon
Utr5
Intron
Utr3
Gene body
RMSK
Other
10M
100K
1K
10

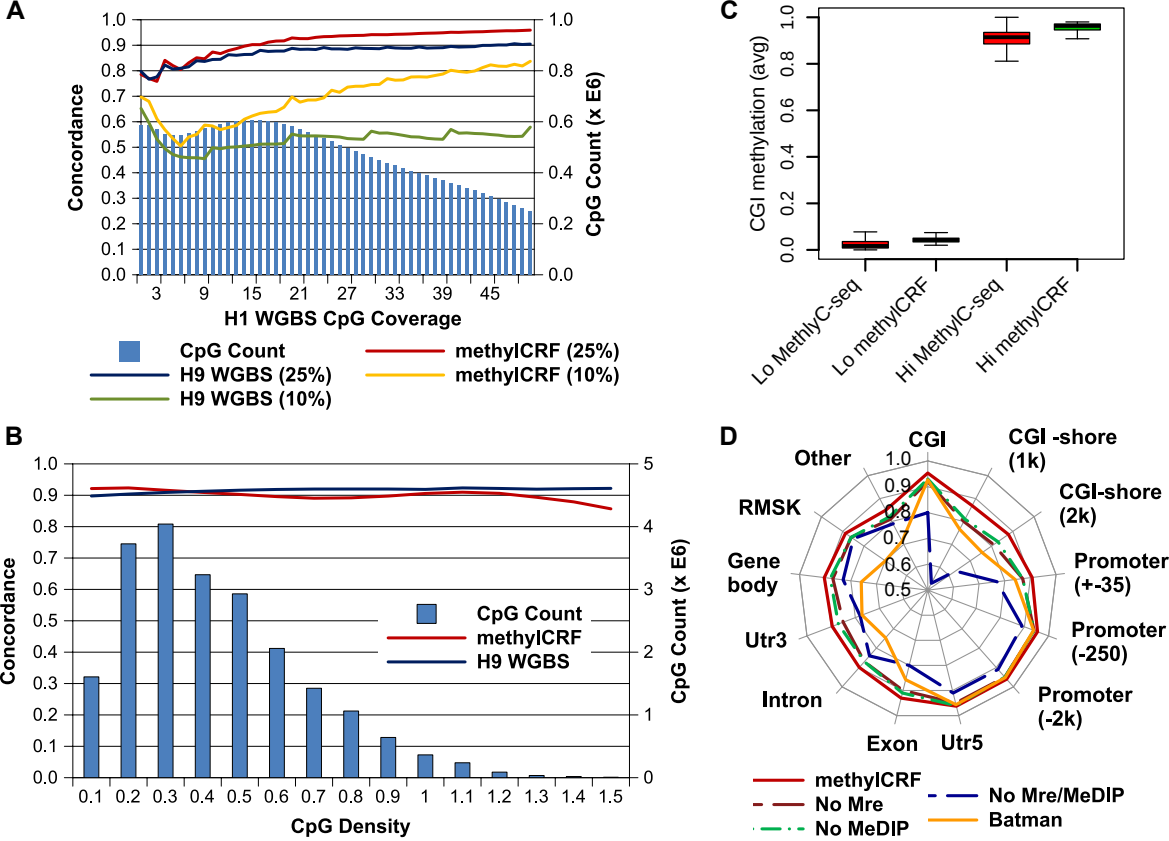
A
Concordance
CpG Count (x E6)
H1 WGBS CpG Coverage
CpG Count
H9 WGBS (25%)
H9 WGBS (10%)
methylCRF (25%)
methylCRF (10%)
B
Concordance
CpG Count (x E6)
CpG Density
CpG Count
methylCRF
H9 WGBS
C
CGI methylation (avg)
Lo MethylC-seq
Lo methylCRF
Hi MethylC-seq
Hi methylCRF
D
CGI
CGI -shore (1k)
CGI-shore (2k)
Promoter (+-35)
Promoter (-250)
Promoter (-2k)
Utr5
Exon
Intron
Utr3
Gene body
RMSK
Other
methylCRF
No Mre
No MeDIP
No Mre/MeDIP
Batman

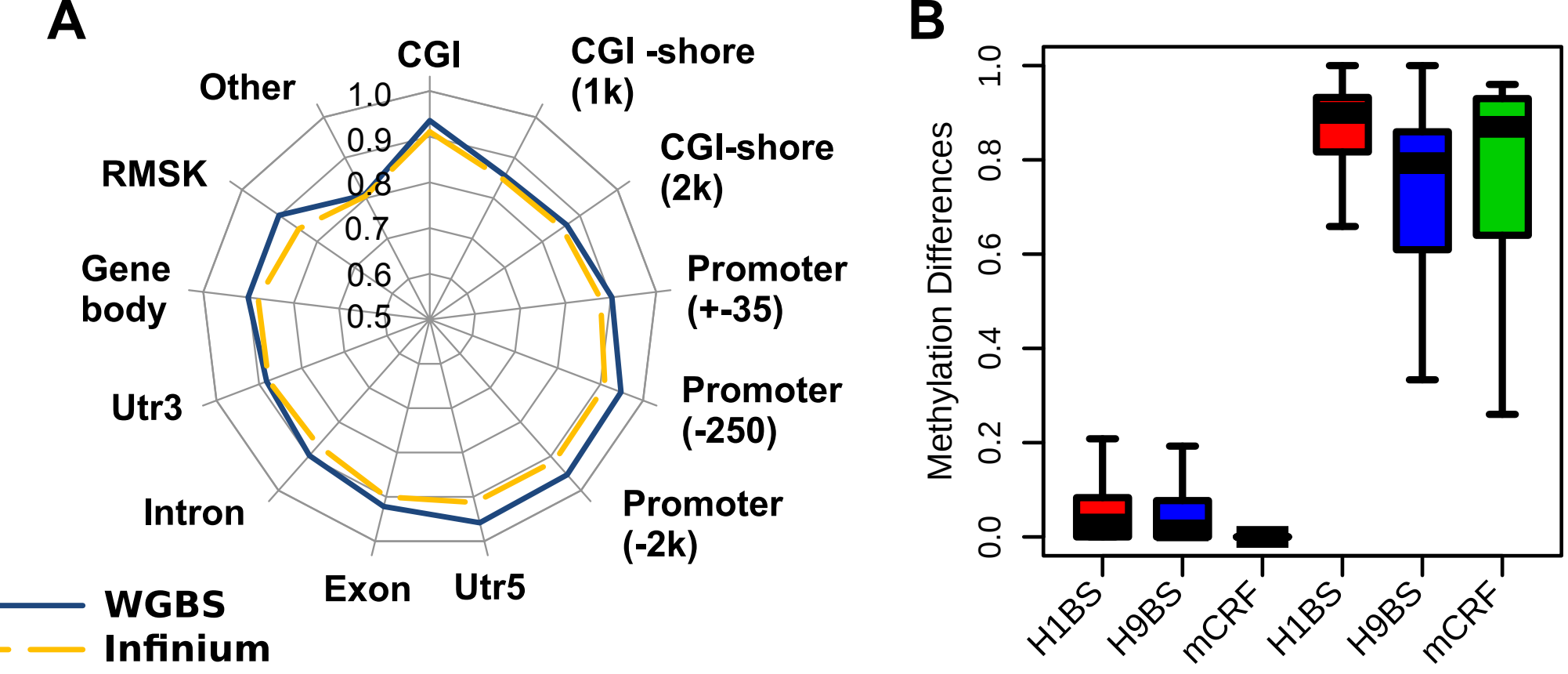
A
CGI
CGI -shore (1k)
CGI-shore (2k)
Promoter (+-35)
Promoter (-250)
Promoter (-2k)
Utr5
Exon
Intron
Utr3
Gene body
RMSK
Other
1.0
0.9
0.8
0.7
0.6
0.5
WGBS
Infinium
B
Methylation Differences
0.0
0.2
0.4
0.6
0.8
1.0
H1BS
H9BS
mCRF
H1BS
H9BS
mCRF

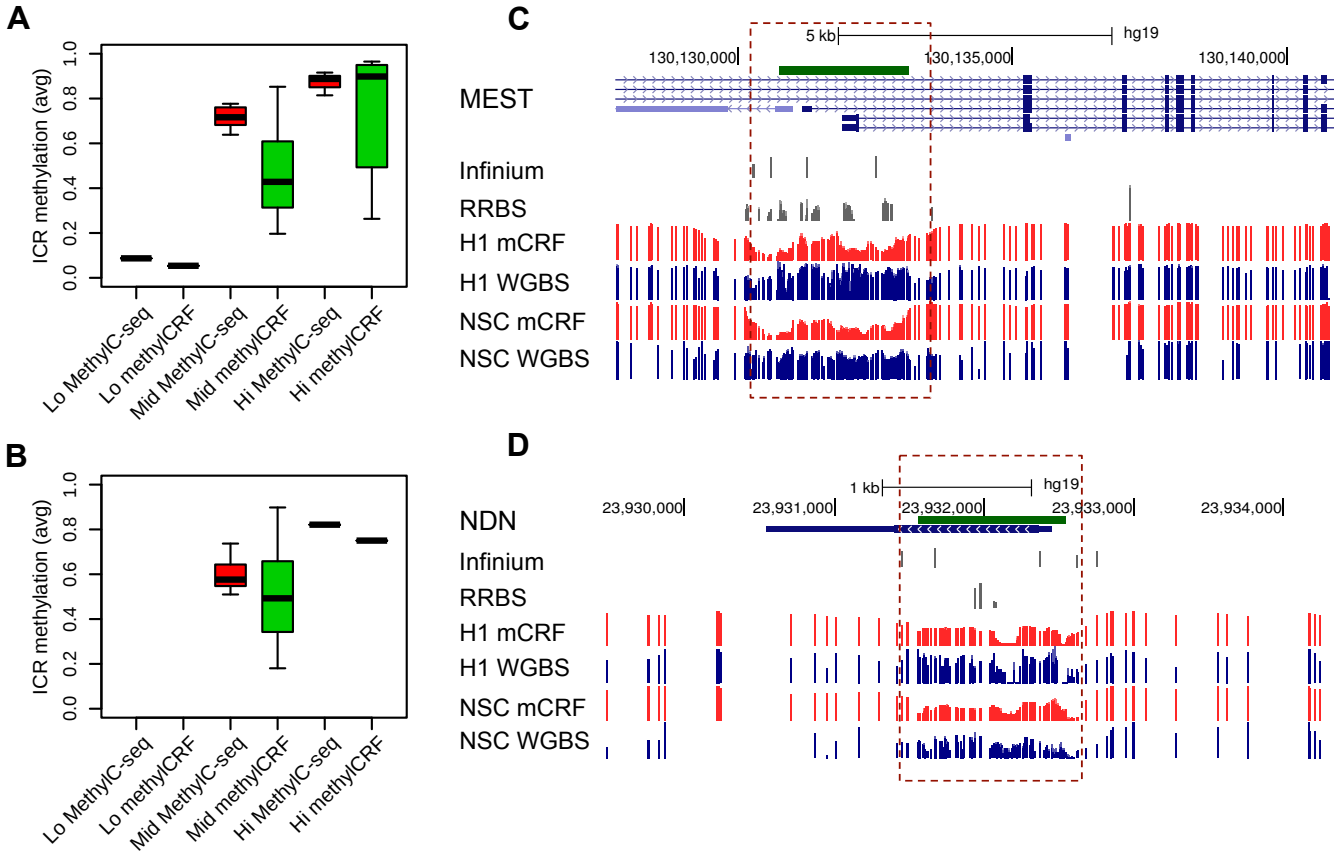
A
ICR methylation (avg)
0.0
0.2
0.4
0.6
0.8
1.0
Lo MethylC-seq
Lo methylCRF
Mid MethylC-seq
Mid methylCRF
Hi MethylC-seq
Hi methylCRF
B
ICR methylation (avg)
0.0
0.2
0.4
0.6
0.8
1.0
Lo MethylC-seq
Lo methylCRF
Mid MethylC-seq
Mid methylCRF
Hi MethylC-seq
Hi methylCRF
C
5 kb
hg19
130,130,000
130,135,000
130,140,000
MEST
Infinium
RRBS
H1 mCRF
H1 WGBS
NSC mCRF
NSC WGBS
D
1 kb
hg19
23,930,000
23,931,000
23,932,000
23,933,000
23,934,000
NDN
Infinium
RRBS
H1 mCRF
H1 WGBS
NSC mCRF
NSC WGBS

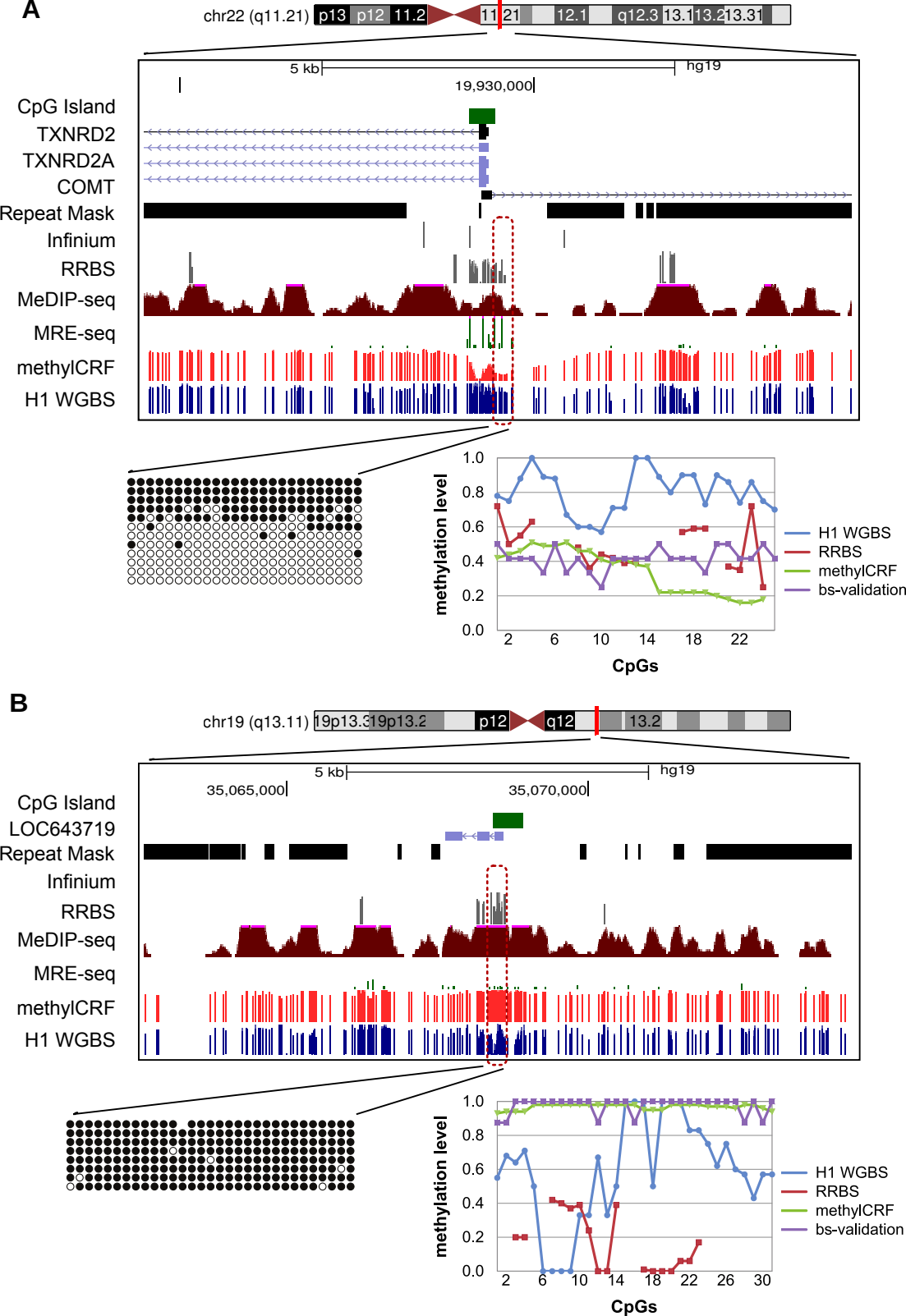
A
chr22 (q11.21)
p13
p12
11.2
11.21
12.1
q12.3
13.1
13.2
13.31
5 kb
hg19
19,930,000
CpG Island
TXNRD2
TXNRD2A
COMT
Repeat Mask
Infinium
RRBS
MeDIP-seq
MRE-seq
methylCRF
H1 WGBS
methylation level
1.0
0.8
0.6
0.4
0.2
0.0
2
6
10
14
18
22
CpGs
H1 WGBS
RRBS
methylCRF
bs-validation
B
chr19 (q13.11)
19p13.3
19p13.2
p12
q12
13.2
5 kb
hg19
35,065,000
35,070,000
CpG Island
LOC643719
Repeat Mask
Infinium
RRBS
MeDIP-seq
MRE-seq
methylCRF
H1 WGBS
methylation level
1.0
0.8
0.6
0.4
0.2
0.0
2
6
10
14
18
22
26
30
CpGs
H1 WGBS
RRBS
methylCRF
bs-validation